International Journal of Pharmaceutics 365 (2009) 121–130

Contents lists available at ScienceDirect

International Journal of Pharmaceutics

journal homepage: www.elsevier.com/locate/ijpharm

Mechanism of action of ZOT-derived peptide AT-1002, a tight junction regulator and absorption enhancer

Shobha Gopalakrishnan, Niranjan Pandey, Amir P. Tamiz, John Vere, Rosa Carrasco, Robert Somerville, Amit Tripathi, Mark Ginski, Blake M. Paterson, Sefik S. Alkan*

Alba Therapeutics, 800 W. Baltimore Street, Suite 400, Baltimore, MD 21201, United States

ARTICLE INFO

Article history:
Received 22 April 2008
Received in revised form 26 July 2008
Accepted 23 August 2008
Available online 11 September 2008

Keywords:
AT-1002
Mechanism of action
Tight junctions
Permeability

ABSTRACT

Tight junctions (TJs) are intercellular structures that control paracellular permeability and epithelial polarity. It is now accepted that TJs are highly dynamic structures that are regulated in response to exogenous and endogenous stimuli. Here, we provide details on the mechanism of action of AT-1002, the active domain of *Vibrio cholerae's* second toxin, zonula occludens toxin (ZOT). AT-1002, a hexamer peptide, caused the redistribution of ZO-1 away from cell junctions as seen by fluorescence microscopy. AT-1002 also activated src and mitogen activated protein (MAP) kinase pathways, increased ZO-1 tyrosine phosphorylation, and rearrangement of actin filaments. Functionally, AT-1002 caused a reversible reduction in transepithelial electrical resistance (TEER) and an increase in lucifer yellow permeability in Caco-2 cell monolayers. *In vivo*, co-administration of salmon calcitonin with 1 mg of AT-1002 resulted in a 5.2-fold increase in AUC over the control group. Our findings provide a mechanistic explanation for AT-1002-induced tight junction disassembly, and demonstrate that AT-1002 can be used for delivery of other agents *in vivo*.

1. Introduction

Tight junctions (TJs) are specialized membrane structures located near the apical aspect of epithelial and endothelial cells. TJs form an intercellular diffusion barrier to regulate the passage of ions, water, and various macromolecules through the paracellular space (reviewed in Aijaz et al., 2006; Hartsock and Nelson, 2008; Schneeberger and Lynch, 2004; Turner, 2006) and form a fence that restricts the mixing of plasma membrane proteins and lipids between the apical and basolateral compartments in cells (Matter and Balda, 1998).

Previously, it was thought that TJs provided a static and immalleable seal of the paracellular space and that patency occurred only with injury, cell death or physico-chemical disruption of the TJ (Nash et al., 1988; Weber and Turner, 2007). It is now understood that TJs are very dynamic structures whose state of assembly changes in a regulated and reversible manner, such that they can open and close to facilitate or restrict paracellular passage of molecules. This implies that TJs can be induced to "leak" and allow transport via paracellular diffusion. There now exists a plethora of data demonstrating that the barrier function of TJs can be modulated by various external and internal stimuli (Shen et al., 2006), both physiologically and as a result of disease or injury (Balda et al., 1991; Bruewer et al., 2003).

TJs are composed of transmembrane proteins occludin, claudins, and junctional adhesion molecules (Furuse et al., 1993, 1998; Martin-Padura et al., 1998), which intercalate with corresponding proteins from adjacent cells to form the intercellular barrier. These proteins associate with an intracellular plaque composed of a variety of peripheral membrane proteins including the membrane associated guanylate kinase (MAGUK) family proteins zonula occludens-1 (ZO-1), -2, and -3 (Haskins et al., 1998; Stevenson et al., 1986), which tether the transmembrane proteins to the underlying actin cytoskeleton and provide a scaffold for intracellular signaling complexes. ZO-1 and occludin phosphorylation are associated with stimulus-induced tight junction disassembly and paracellular permeability changes (Sheth et al., 2003; Staddon et al., 1995; Takeda and Tsukita, 1995).

Since the 1960s efforts to develop TJ-based absorption enhancers have focused primarily on calcium chelators and surfactants, which have failed due to unacceptable side effects such as exfoliation of epithelia and irreversibility of barrier disruption (Hochman and Artursson, 1994). More recent investigations have focused on bile salt components, mucoadhesive polymers such

Abbreviations: TJ, tight junction; TEER, transepithelial electrical resistance; LY, lucifer yellow; ZOT, zonula occludens toxin from *V. cholerae*; pMLC, phospho-myosin light chain; MAGUK, membrane associated guanylate kinase; MAP kinase, mitogen activated protein kinase.

* Corresponding author. Tel.: +1 410 319 0858; fax: +1 410 244 8616.
E-mail address: salkan@albatherapeutics.com (S.S. Alkan).

0378-5173/$ – see front matter © 2008 Elsevier B.V. All rights reserved.
doi:10.1016/j.ijpharm.2008.08.047

as chitosans, and peptidic antagonists/modulators of occludin and claudin, but these efforts have also generally failed to yield candidates for clinical development (Kondoh and Yagi, 2007). However, the progress in understanding of TJ cell biology described above and the observed reversibility and reproducibility of TJ signal transduction has led us to explore TJ regulation as a target for drug development.

Vibrio cholerae secretes zonula occludens toxin (ZOT), which binds to a putative receptor on the apical surface of enterocytes (Baudry et al., 1992; Fasano et al., 1991; Lee et al., 2003; Schmidt et al., 2007) and induces a transient reduction in TEER and an increase in trans-epithelial flux along concentration gradients (Lee et al., 2003). ZOT-induced mucosal permeability has been utilized experimentally to transport diverse macromolecules, such as insulin and paclitaxel, resulting in a significant increase in bioavailability and a therapeutic effect across various mucosal surfaces and the blood brain barrier (Fasano and Uzzau, 1997; Salama et al., 2004, 2005, 2006). It has also been useful in inducing persistent and protective mucosal immunity (De Magistris, 2006; Marinaro et al., 1999, 2003). ZOT has been reported to increase permeability of the small intestinal mucosa by inducing cytoskeletal contraction, which affects TJs (Fasano et al., 1995). Delta G, the 12 kDa active fragment of ZOT, has been shown to transiently increase the *in vitro* transport and *in vivo* absorption of paracellular markers (Lee et al., 2003; Salama et al., 2004, 2005, 2006).

Cholera toxin, ZOT and other agents of prokaryotic origin may not be suitable adjuvants due to their complex structures, problems with expression and purification (Schmidt et al., 2007), antigenicity and possible ganglioside binding. To avoid problems associated with these large prokaryotic molecules, a synthetic peptide H-FCIGRL-OH (AT-1002) that comprises the first six amino acids of Delta G and retains the permeability enhancing effects of Delta G on TJs (Di Pierro et al., 2001; Motlekar et al., 2006) has recently been identified and synthesized. The purpose of this study was to evaluate the effects of AT-1002 on epithelial TJ assembly, barrier function and *in vivo* drug delivery. We examine signaling events initiated by AT-1002 that ultimately lead to tight junction opening and drug delivery, and also demonstrate reversible TJ modulation by AT-1002.

2. Materials and methods

2.1. Reagents

AT-1002 was synthesized using F-moc solid phase chemistry. Individual steps such as coupling, deprotection, and cleavage were performed following a reported protocol (Cammish and Kates, 2000), and the identity of the compound was confirmed by LC/MS. The final product was isolated as a TFA salt in a lyophilized form. For *in vivo* studies, AT-1002 was isolated as an HCl salt using established methods.

A wide range of AT-1002 concentrations was tested on several cell lines. The most consistent and reproducible results were obtained with 5 mg/ml of peptide. In addition, several scrambled or unrelated hexamer peptides tested at 5 mg/ml had no biological activity (Table 1). After making sure that effects of the AT-1002 at this dose were specific, this concentration (5 mg/ml) was used throughout this study.

Table 1
Summary of results obtained with scrambled and unrelated peptides

Compound	Sequence	LY permeability enhancement (5 mg/ml)	ZO-1 reorganization (5 mg/ml)
AT-1002	FCIGRL	14.7	+++
Scrambled peptide-1	GFGILR	–	–
Scrambled peptide-2	IGFLRG	–	–
Unrelated peptide-1	QLYENK	–	–
Unrelated peptide-1	KNPYIL	–	–

2.2. Cell lines and treatment

Intestinal epithelial IEC6 cells were obtained from American Type Culture Collection (ATCC; Manassas, VA) and maintained in DMEM containing 0.1 unit/ml bovine insulin, 10% fetal bovine serum, penicillin (100 unit/ml) and streptomycin (100 μg/ml). These cells were used for immunofluorescence studies, but not for permeability studies because they do not form functional tight junctions.

Caco-2 cells were obtained from ATCC and maintained in DMEM containing non-essential amino acids, 10% fetal bovine serum, penicillin (100 units/ml) and streptomycin (100 μg/ml). Cells were plated at 100,000 cells per 12-well filter and used at 20–22 days post-plating. This cell line was mainly used for permeability studies.

Caco-2 BBE cells were obtained from ATCC and maintained in DMEM containing 0.1 mg/ml human transferrin, 10% fetal bovine serum, penicillin (100 units/ml) and streptomycin (100 μg/ml). Cells were plated at 100,000 cells per 12-well filter and used at 10–15 days post-plating. These cells were used for immunofluorescence and biochemical studies because they are more homogenous than regular Caco-2 cells and the monolayers they form on filters can be readily imaged.

2.3. Immunofluorescence

IEC6 cells were plated on 8-chamber slides at 60,000 cells per chamber. At 24 h post-plating, cells were washed in serum-free medium and incubated with AT-1002 (5 mg/ml) diluted in serum-free medium for 60 min at 37 °C. Following treatment, cells were washed in PBS and fixed in PBS containing 4% paraformaldehyde for 15 min at room temperature. Cells were washed in PBS, permeabilized in PBS containing 0.5% Triton X-100 for 5 min at room temperature, and blocked in PBS containing 2% goat serum for 30 min at room temperature. Cells were then incubated with primary antibodies diluted in blocking buffer (pMLC (1:50) (Cell Signaling technology, Danvers, MA)) for 1–2 h at 37 °C. Cells were washed in PBS and incubated with FITC tagged anti-rabbit antibody (1:100; Jackson Immunoresearch, Bar Harbor, ME) for 45 min at room temperature. Actin and ZO-1 were detected using Alexa Fluor555-phalloidin and FITC labeled anti-ZO-1 antibodies (1:200; Invitrogen, Carlsbad, CA), respectively. Slides were washed and mounted in Vectashield containing DAPI and imaged on a Nikon-TE2000 fluorescence microscope.

Caco-2 BBE cells were treated apically with AT-1002 (5 mg/ml) for 3 h at 37 °C. Following treatment cells were fixed in methanol:acetone (1:1) and blocked in PBS containing 2% goat serum. Filters were incubated with FITC labeled anti-ZO-1 antibodies (1:200; Invitrogen, Carlsbad, CA) for 1 h at room temperature, washed and mounted on slides as described above.

For ZO-1, a *z*-series of *x*–*y* images through the entire cell volume of the monolayer was collected and combined into a single projection image to avoid missing fluorescent signal from out-of-focus planes. Junctional fluorescence intensity of ZO-1 was quantified using Adobe Photoshop as follows. Background level was adjusted using the threshold function. Then the brightness was adjusted to bring all background pixels to the threshold value. Pixels at cell–cell junctions were highlighted using the Magic wand and select/inverse functions. The mean pixel intensity value, total number of pixels and number of threshold pixels were obtained

from the histogram. Total junctional fluorescence intensity = (total pixels × mean pixel value) − (threshold pixels × threshold) was calculated for each sample.

2.4. Flow cytometry

Caco-2 BBE cells were treated apically with AT-1002 (5 mg/ml) for 3 h at 37 °C. Following treatment cells were detached from filters using trypsin. Detached cells were washed in PBS, fixed in PBS containing 4% paraformaldehyde for 15 min at room temperature, permeabilized in PBS containing 0.5% Triton X-100 for 5 min at room temperature, and blocked in PBS containing 2% goat serum for 30 min at room temperature. Cells were incubated with Alexa Fluor555-phalloidin for 1 h at room temperature, washed in PBS and analyzed by flow cytometry using FACSCAN (Becton Dickinson, San Diego, CA).

2.5. Immunoprecipitation

Caco-2 BBE cell cultures were rinsed with ice-cold phosphate-buffered saline. Cells were extracted with RIPA buffer (150 mM NaCl, 1% IGEPAL, 0.5% deoxycholate, 0.1% SDS, phosphatase and protease inhibitors) for 15 min on ice. Extracts were cleared by centrifugation in a microfuge at 13,000 rpm for 15 min at 4 °C. Primary antibody (ZO-1 polyclonal antibody, Invitrogen, CA) was added to supernatants, and tubes were rotated at 4 °C for 16 h. Immune complexes were collected with protein A-Sepharose beads (Amersham, Piscataway, NJ) and washed three times with RIPA buffer. Beads were resuspended in SDS sample buffer for analysis, and separated on 4–12% or 10% Bis–Tris gels (Invitrogen, CA). Immunoblotting was performed as described in the following section.

2.6. Immunoblotting

Caco-2 BBE cells were treated with permeability inducer for 60 min or left untreated in control dishes. Cultures were then extracted in RIPA buffer. Samples were cleared by centrifugation. Protein concentration of supernatants was determined using a bicinchoninic acid (BCA) protein assay kit (Pierce Chemical, Rockford, IL). Twenty micrograms of protein were separated on 4–12% or 10% Bis–Tris gels (Invitrogen). Gels were transferred to nitrocellulose filters (Bio-Rad, Hercules, CA) and blocked in membrane blocking buffer (Invitrogen, CA) for ZO-1 or Tris-buffered saline containing Tween 20 and 1% BSA (TBST: 10 mM Tris–HCl, pH 7.5, 100 mM NaCl, and 0.1% Tween 20) for phosphotyrosine, or TBST containing 5% milk for other proteins at 4 °C overnight. Filters were incubated in primary antibody (ZO-1, (Invitrogen, CA), src and Tyr416-src (Cell Signaling Technology, MA) (1:1000 each)) for 1 h at room temperature, and blots were then washed in TBST for 1 h with several changes. Membranes were then incubated for 1 h at room temperature with species-matched HRP-conjugated secondary antibody (Amersham, Arlington Heights, IL) diluted 1:5000 in blocking solution or HRP-conjugated phosphotyrosine (1:1000) in blocking solution. Membranes were again washed, and signal was detected by enhanced chemiluminescence (ECL kit; Amersham, Arlington Heights, IL) and exposed to film (Kodak Bio-Max ML; Eastman Kodak, Rochester, NY). Relative phosphorylation levels were quantified using ImageQuant TL software (Amersham).

2.7. In vitro cytotoxicity assays

Cell viability was determined by measuring the amount of ATP in cells using a luminescence ATP assay (CellTiter-Glo Promega, Madison, WI). The concentration of ATP is determined by the amount of light emitted when beetle luciferin is mono-oxygenated by luciferase in a reaction that is Mg^{2+} and ATP-dependent. A range of concentrations of AT-1002 from 0 to 5 mg/ml in 100 μl of Hank's Balanced Salt Solution (HBSS) was added to 30,000 Caco-2 cells grown on 96-well tissue culture plates after removal of the growth media. An equal volume of Cell titer-Glo reagent was added to the wells after 3 h and the chemiluminescence was measured after 15 min incubation in a Tecan Spectrafluor plus plate reader. A standard curve was generated for ATP and used to calculate the concentration of ATP after treatment with AT-1002.

2.8. TEER and lucifer yellow permeability assays

Details of this method and modifications have been described previously (Artursson, 1990; Ginski and Polli, 1999). For transepithelial electrical resistance (TEER) and lucifer yellow (LY) permeability assays, Caco-2 cells were seeded onto 12-well Transwells™ (Corning Inc., NY, polyester, pore size 0.4 μm) at a density of 100,000 cells/cm^2 and grown for 21–28 days until fully differentiated. The apical and basolateral compartments of the Caco-2 cell monolayers were pre-incubated in HBSS at 37 °C for 30 min. Treatment solutions containing a range of concentrations of AT-1002 from 0.4 to 5 mg/ml AT-1002 or 5 mg/ml scrambled peptide in HBSS were added to the apical compartment of each monolayer and then incubated at 37 °C, 50 rpm for 180 min. TEER was measured using a MilliCell-ERS at 0, 30, 60, 120 and 180 min. At 180 min, AT-1002 was replaced in the apical compartment by 7.5 mM lucifer yellow. After 1 h incubation at 37 °C, samples were removed from the basolateral compartment and analyzed for LY in a Tecan Spectrofluor fluorescence plate reader at excitation wavelength of 485 nm and emission wavelength of 535 nm. The decrease in TEER and increase in LY permeability was calculated for each treatment and expressed relative to lucifer yellow untreated control. The permeability is calculated as follows: $\text{Papp} = [(dC/dt) \times V_r]/(C_o \times A)$, where dC/dt is the permeability rate, V_r is the volume of the receiver, A is the surface area of the membrane filter, and C_o is the initial concentration in the donor chamber, and the enhancement ratio is defined as Papp AT-1002/Papp HBSS.

2.9. Reversibility of AT-1002 effects on Caco-2 cells

Caco-2 cells were seeded on transwell membranes as described above and grown in DMEM for a period of 21 days at 37 °C, 5% CO_2 and 95% humidity with medium change every other day. At the end of the growth period the medium from the upper (apical) and lower (basolateral) compartments was removed. The cells were incubated in pre-warmed (37 °C) HBSS (Mediatech, Inc., Herndon, VA, USA) (with Ca and Mg) with 10 mM HEPES pH 7.4. The transwells were treated apically with or without AT-1002 at a concentration of 5 mg/ml in HBSS for various times. The AT-1002 was either replaced by HBSS after 15, 30, 45 and 60 min or not removed at all. TEER readings were monitored using an Ohm meter (World Precision Instruments Inc., Saratosa, FL, USA) at different time points.

2.10. Intratracheal delivery of salmon calcitonin

We conducted *in vivo* pulmonary drug delivery study in rats with IACUC approval and IACUC Protocol 05-01A. Male Sprague–Dawley rats were used for this study and were approximately 12 weeks of age at the initiation of the study. All rats were instilled intratracheally with 10 μg of sCT in 200 μl of saline containing 0, 300 or 1000 μg of AT-1002 ($n = 6$ per dose group). Blood samples (200 μl) were collected and placed into EDTA coated tubes prior to dosing and at 2.5, 5, 10, 15, 30, 60, 120 and 240 min following dosing. Plasma was harvested and stored at ≤−70 °C until assayed for sCT. The DSL 10–3600 ACTIVE® Salmon Calcitonin Enzyme-Linked

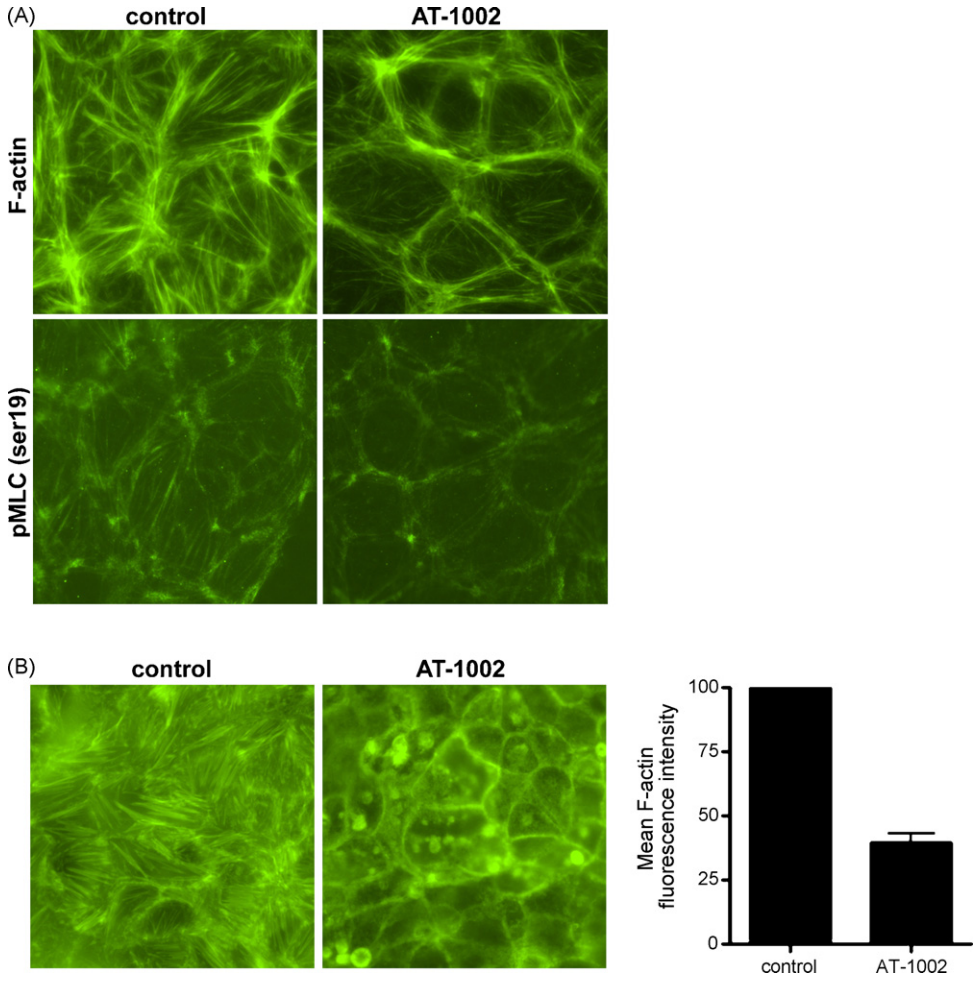

Fig. 1. Effect of AT-1002 on the actin cytoskeleton in IEC6 and Caco-2 BBE cells. IEC6 (A) or Caco-2 BBE cells (B) were treated with AT-1002 for 1 h. Cells were fixed and processed by immunofluorescence to detect F-actin and pMLC (A). Following AT-1002 treatment, cells were fixed on filters or dissociated from membranes and processed by immunofluorescence to detect F-actin by microscopy or FACS (B, right panel), respectively. Values are mean ± S.D. Data are representative of three independent experiments.

Immunosorbent (ELISA) kit was used with slight modifications to determine concentrations of sCT in rat plasma. This assay is an enzymatically amplified "two-step" sandwich-type immunoassay involving the biotin-streptavidin bridging detection system. For these studies standards were prepared in a rat serum matrix and the curve ranged from 15.6 to 1000 pg/ml. The LLOQ was 31.3 pg/ml. The sample volume used was 50 μl. When necessary, samples (concentrations expected or measured above 1000 pg/ml) were diluted with the rat serum matrix. Standard curves were calculated using a four parameter fit model using the KC4 software available on a BioTek Plate reader. Assay performance did not appear to be influenced by the difference between the sample (rat plasma) and standard (rat serum) matrix. Microsoft Excel® was used for calculation of AUC using the linear trapezoidal rule and data were plotted using GraphPad Prism version 4.01. C_{max} and T_{max} for each condition were also determined. Statistical analyses were conducted using SAS® for Windows Version 9.1.

3. Results

3.1. Actin dynamics in IEC6 and Caco-2 cells

Both ZOT and its active fragment Delta G cause cytoskeletal rearrangement as an integral component of the signaling leading to TJ modulation (Fasano et al., 1995; Salama et al., 2004; Schmidt et al., 2007). To determine whether AT-1002 exerts a similar effect on the actin cytoskeleton, IEC6 cells were treated for 1 h with AT-1002 diluted in serum-free medium or serum-free medium alone and the actin cytoskeleton was visualized by immunofluorescence using fluorescent phalloidin and anti-pMLC antibody. AT-1002 caused cytoskeletal redistribution, with dissolution of central stress fibers and stress-fiber associated pMLC (Fig. 1A). Effect of AT-1002 on the actin cytoskeleton was also examined in Caco-2 BBE cells by microscopy and flow cytometry. Similar to that in IEC6 cells, AT-1002 caused disassembly of stress fibers in Caco-2 cells and a decrease in F-actin content to 40% of control levels (Fig. 1B).

3.2. ZO-1 distribution in Caco-2 cells

The effect of AT-1002 on TJ integrity was studied in Caco-2 BBE cells by immunofluorescence. A *z*-series of *x*–*y* images through the entire cell volume of the monolayer was collected and combined into a single projection image and junctional fluorescence intensity of ZO-1 was quantified. In untreated cells ZO-1 is seen as the typical "chicken wire" staining characterized by smooth lines at cell–cell junctions. AT-1002 caused loss of ZO-1 from sites of cell–cell contact (Fig. 2A). Junctional fluorescence intensity of ZO-1 decreased to 40% that of control levels following AT-1002 treatment (Fig. 2A). No change in ZO-1 distribution was seen with the scrambled peptide controls (Fig. 2B).

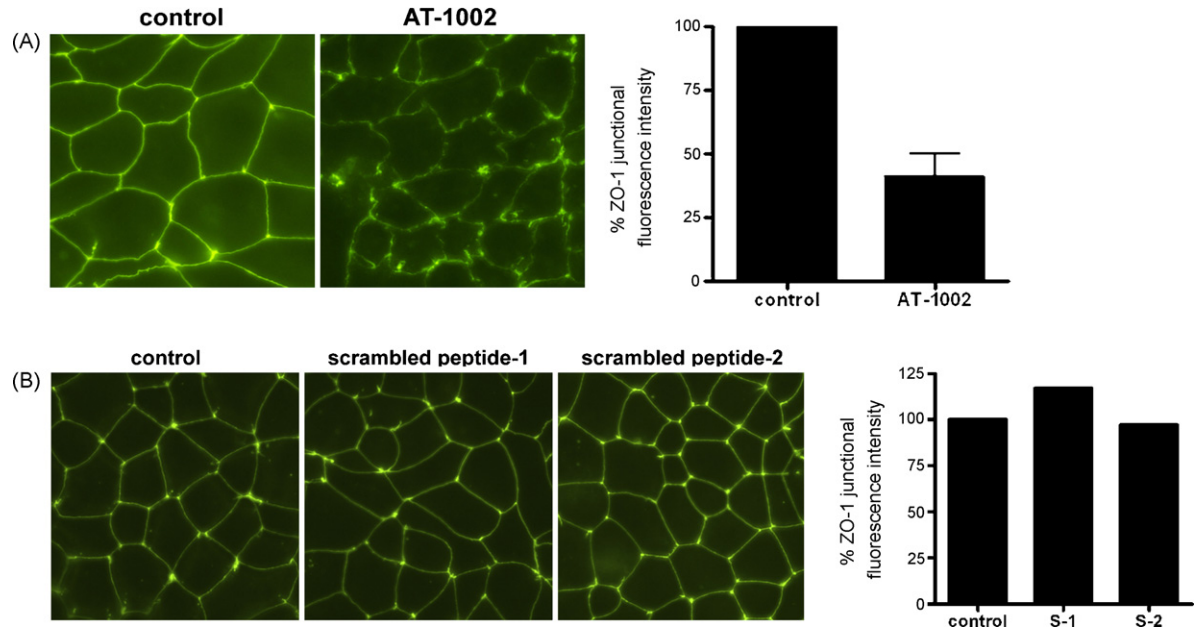

Fig. 2. Effect of AT-1002 on ZO-1 distribution in Caco-2 BBE cells. Caco-2 BBE cells grown on permeable filter supports were treated apically with AT-1002 for 3 h. Cells were then fixed and processed by indirect immunofluorescence using antibodies against ZO-1 (A). Scrambled versions of AT-1002 (S-1 and S-2) were tested for ZO-1 redistribution in Caco-2 BBE cells at 5 mg/ml (B). Fluorescent images were quantified using Adobe Photoshop. Values are mean ± S.D. Data are representative of three independent experiments.

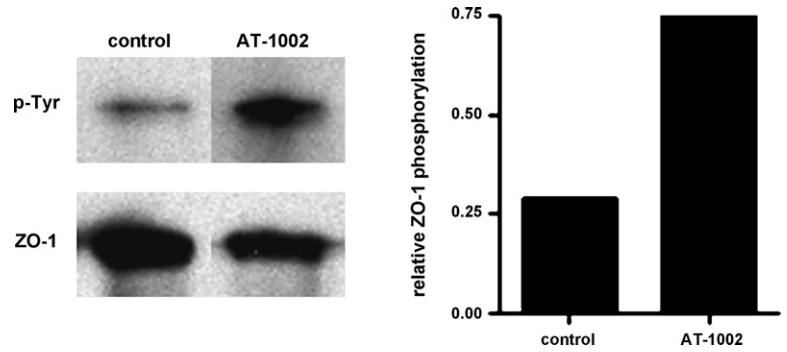

Fig. 3. Effect of AT-1002 on tyrosine phosphorylation of ZO-1 in Caco-2 BBE cells. Caco-2 BBE cells were treated with AT-1002 for 3 h. ZO-1 was immunoprecipitated from treated and untreated cells, separated by gel electrophoresis, transferred to nitrocellulose and immunoblotted with antibodies against phosphotyrosine or ZO-1. Data are representative of three independent experiments.

3.3. TJ signaling events

ZO-1 is a phosphoprotein and changes in phosphorylation of TJ proteins have been shown to accompany increases in permeability (Staddon et al., 1995; Takeda and Tsukita, 1995). To examine the effects of AT-1002 on ZO-1 tyrosine phosphorylation, ZO-1 was immunoprecipitated from either untreated or AT-1002-treated Caco-2 cell extracts, and the phosphotyrosine content was examined by immunoblotting the immunoprecipitates with a phosphotyrosine antibody. AT-1002 treatment resulted in 3-fold increase in phosphotyrosine content of ZO-1 (Fig. 3).

Src family kinases associate with TJs (Anderson and Van Itallie, 1995). Increased tyrosine phosphorylation of ZO-1 may therefore be a consequence of src kinase activation. We examined the effects of AT-1002 on src activation by western blotting using a phospho-specific anti-src antibody in Caco-2 cells. AT-1002

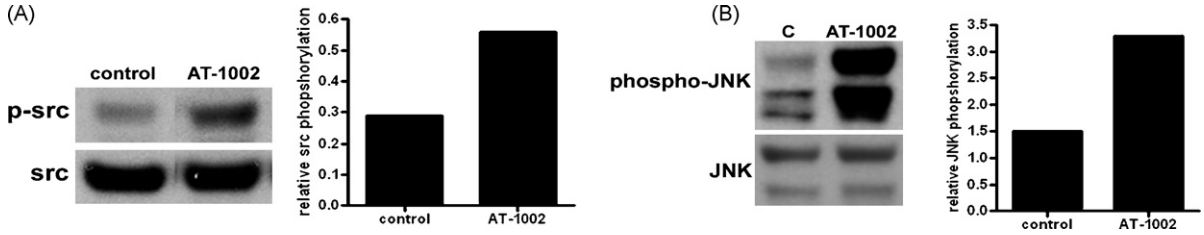

Fig. 4. Effect of AT-1002 on src and MAP kinase activation in Caco-2 BBE cells. Caco-2 BBE cells were treated with AT-1002 for 1 h (for src) or 3 h (for MAP kinase) and extracted with RIPA buffer. Equal amounts of protein from treated and untreated samples were separated by gel electrophoresis and immunoblotted with antibodies against (A) total src, phospho-src, or (B) total JNK or phospho-JNK. Data are representative of three independent experiments.

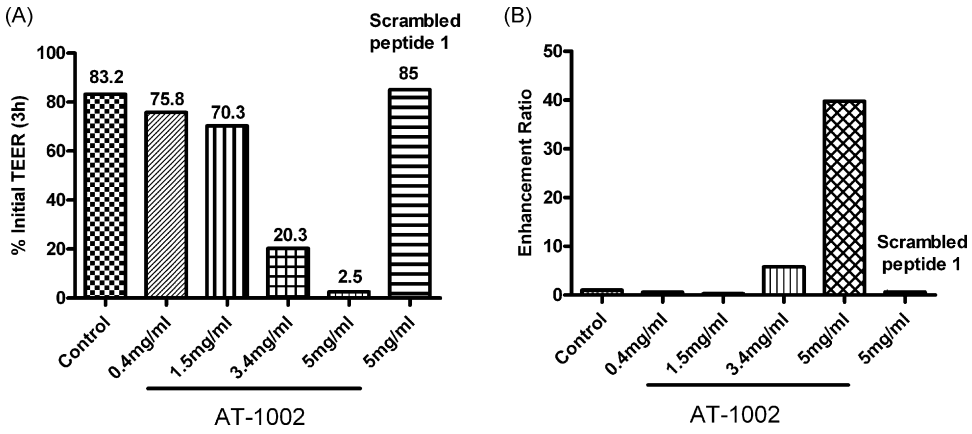

Fig. 5. Effect of AT-1002 on TEER and LY permeability. Caco-2 cells grown on permeable filter supports were treated apically with AT-1002 or a scrambled version of AT-1002 and (A) TEER was monitored at 3 h. (B) Treated and untreated cells were incubated with LY for another 1 h and permeability was measured as described in Section 2. Data are representative of three independent experiments.

increased phosphorylation of src on tyr416 in Caco-2 cells (Fig. 4A). AT-1002 also caused src activation in IEC6 cells (data not shown).

Activation of mitogen activated protein kinase (MAP kinase) signaling pathways is associated with TJ opening in response to various stimuli (Chen et al., 2000; Patrick et al., 2006). We therefore examined activation of the MAP kinase pathway in Caco-2 cells following AT-1002 treatment by immunoblotting cell extracts with phospho-specific anti-MAP kinase antibodies. AT-1002 caused activation of c-jun N-terminal (JNK) kinase (Fig. 4B), as well as extracellular signal regulated 1/2 (ERK1/2) and p38 MAP kinases (data not shown).

3.4. Barrier function

We examined the effects of AT-1002 on TEER and permeability in Caco-2 cell monolayers, a widely used model for barrier function studies. Cells grown on permeable supports were treated apically for 3 h with AT-1002 or left untreated for the control. TEER across cell monolayers was measured following exposure to AT-1002. TEER values remained unchanged in the presence of the vehicle control and scrambled peptide, whereas TEER decreased in a dose dependent fashion in the presence of AT-1002 (Fig. 5A). Changes in paracellular permeability across Caco-2 cell monolayers in response to AT-1002 were measured using lucifer yellow. LY permeability remained unchanged in the presence of vehicle control, whereas it increased substantially in response to AT-1002 (Fig. 5B). In contrast, a scrambled version of AT-1002 did not reduce TEER (Fig. 5A) or increase permeability of the Caco-2 monolayer (Fig. 5B) when tested at a dose of 5 mg/ml.

3.5. In vitro cell viability assays

To rule out the possibility that AT-1002-induced cytoskeletal changes and increases in permeability are the result of cytotoxicity, we examined the effect of AT-1002 on Caco-2 cell viability. Undifferentiated Caco-2 cells were treated with AT-1002 and viability was assessed by measuring cellular ATP content. Treatment with AT-1002 for up to 3 h did not affect cell viability at any concentration. In particular, the viability of Caco-2 cells was not affected by 5 mg/ml AT-1002 (Fig. 6), the concentration used in the other cell-based assays described here. AT-1002 did reduce cell viability after 24 h at concentrations of 2.5 mg/ml and higher. However, the cells remained viable after 24 h if the cells were washed after exposure to AT-1002 for 3 h indicating that AT-1002 did not irreversibly damage cells.

3.6. Reversibility assays

Next we tested the reversibility of AT-1002 induced decrease in TEER of a Caco-2 monolayer. In this experiment, Caco-2 monolayers were left untreated or treated with 5 mg/ml AT-1002 for 15, 45, and 60 min or for 24 h. All the monolayers except the 24 h time point were allowed to recover in the absence of AT-1002. By 60 min TEER dropped to 25% of control values in all groups (Fig. 7A). TEER values started to recover within 2 h in the monolayers that had been exposed to AT-1002 for 15, 45 and 60 min and recovery was complete between 6 and 23 h after removal of AT-1002. The kinetics of TEER recovery depended on the duration of exposure to AT-1002. Specifically, cells that were exposed to AT-1002 for 15 min recovered earlier and the recovered TEER values were higher than those for monolayers that were exposed to AT-1002 for 30, 45 or 60 min. The monolayers that were exposed to AT-1002 for 24 h had recovered TEER only slightly by the end of the incubation. This could be due to decrease in cell viability after a 24 h incubation with AT-1002 (Fig. 6). However, it is known that *in vivo* AT-1002 does not persist in its original/intact form for longer than 60 min (Li et al., 2008). In addition, in an intravenous push study in rats no signs of toxicity were observed at up to 50 mg/kg of AT-1002 (unpublished observations).

We also examined the reversibility of AT-1002 induced increase in phosphotyrosine content of ZO-1. Here, Caco-2 cells were treated with 5 mg/ml AT-1002 for 30 min. After removal of AT-1002 cells were incubated in regular growth medium for 2 h. ZO-1 was immunoprecipitated from untreated and AT-1002 treated cells with

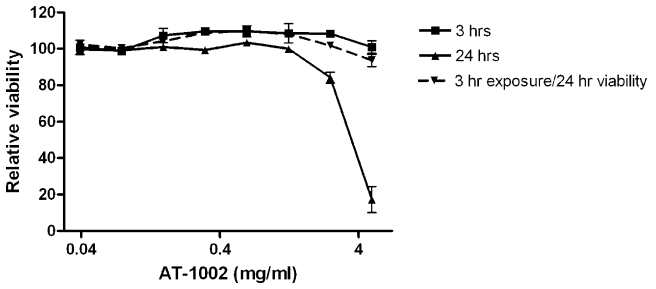

Fig. 6. Effect of AT-1002 on Caco-2 cell viability. Caco-2 cells grown in 96-well tissue culture plates were treated with a range of concentrations from 0 to 5 mg/ml of AT-1002 for 3 or 24 h or washed after exposure to AT-1002 for 3 h. After the indicated times cell viability was determined by measuring the levels of ATP in the cells using the Cell titer-Glo assay kit. Values are mean ± S.D.

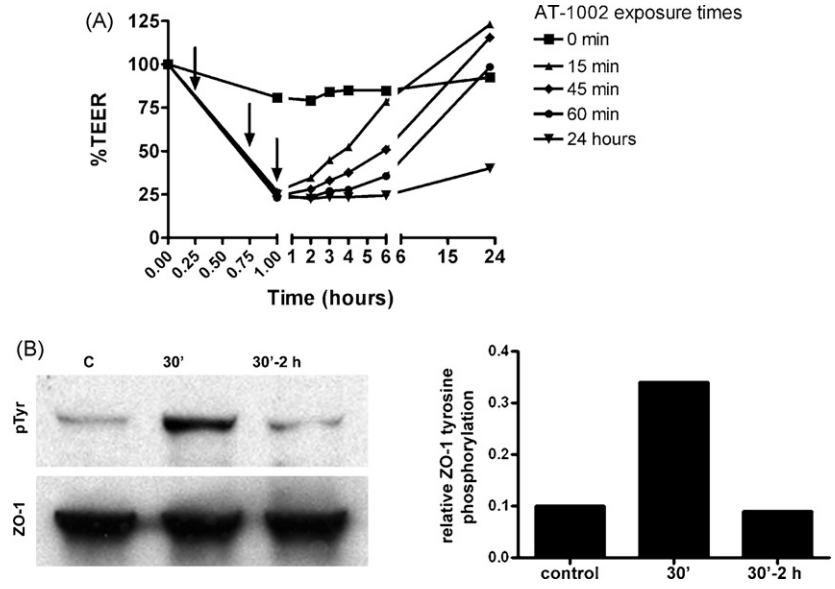

Fig. 7. Reversible nature of the activity of AT-1002. (A) Caco-2 cells grown on filter supports were treated apically with or without AT-1002 at a concentration of 5 mg/ml in HBSS. The AT-1002 was either replaced by HBSS after 15, 30, 45 and 60 min or not removed at all. The TEER readings were monitored using an Ohm meter at the indicated time points. The arrows indicate the 15, 45 and 60 min agonist removal times. Data are representative of two independent experiments. (B) Caco-2 cells grown on filter supports were treated with AT-1002 for 30 min and allowed to recover for 2 h in the absence of AT-1002. ZO-1 was immunoprecipitated from treated and untreated cells, separated by gel electrophoresis, transferred to nitrocellulose and immunoblotted with antibodies against phosphotyrosine or ZO-1. Data are representative of two independent experiments.

or without recovery, and immunoprecipitates were analyzed for phosphotyrosine by immunoblotting. AT-1002 caused an increase in ZO-1 tyrosine phosphorylation within 30 min (Fig. 7B). When cells were allowed to recover for 2 h in the absence of AT-1002, tyrosine phosphorylation levels of ZO-1 returned to control levels, indicating that the AT-1002 induced increase in ZO-1 phosphorylation was reversible.

3.7. *In vivo* activities

It was of great interest to determine if the *in vitro* effects of AT-1002 described above could be translated into *in vivo* effects. Previously it has been shown that AT-1002 was able to increase the delivery of payloads administered into the gastrointestinal system *in vivo* (Motlekar et al., 2006; Song et al., 2008a, 2008b). Here we wanted to determine if AT-1002 could enhance delivery of payloads applied to the airway epithelia. Thus, we tested whether AT-1002 could increase the systemic exposure of salmon calcitonin (sCT), which by itself has very low bioavailability. Intratracheal instillation of 10 μg of sCT with increasing amounts of AT-1002 into rats resulted in increased pulmonary absorption and higher systemic concentrations of sCT in the treatment groups with the highest amount of AT-1002 (Fig. 8). When sCT was administered 2 h after the AT-1002 administration, no enhanced absorption was observed indicating that the effect of AT-1002 was transient (data not shown). No differences were observed among pharmacokinetic parameters below a delivered dose of 300 μg of AT-1002 (data not shown). The sCT $AUC_{0-240\ min}$ was significantly increased

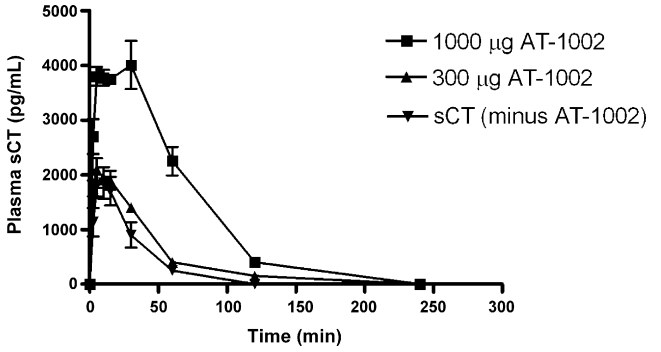

Fig. 8. Effect of doses of AT-1002 (μg) on pulmonary absorption of sCT following liquid instillation of both AT-1002 and salmon calcitonin (sCT). Rats were instilled with saline or saline with 0, 300, or 1000 μg AT-1002 ($n = 6$) together with 10 μg sCT. Blood samples (200 μl) were collected and placed into EDTA coated tubes prior to dosing and at 2.5, 5, 10, 15, 30, 60, 120 and 240 min following dosing. Plasma was harvested and stored at ≤−70 °C until assayed for sCT by ELISA. C_{max}, T_{max}, $AUC_{0-240\ min}$, and relative % of AUC to control are reported. Values are mean ± S.D.

over the control group (0 μg dose) at 300 and 1000 μg of AT-1002 (Table 2). Co-administration of sCT with 300 and 1000 μg of AT-1002 resulted in a 1.6-fold (161.8%) and 5.2-fold (522.5%) increase in AUC over the control group, respectively. C_{max}, which is a measure of the highest concentration achieved, was also 2.3-fold higher when 1000 μg of AT-1002 was co-administered with sCT relative to control.

Table 2
Summary of pharmacokinetic parameters of co-administration of AT-1002 with salmon calcitonin (sCT)

Dose delivered AT-1002 (μg/ml)	*n*	C_{max} (pg/ml) (±S.D.)	T_{max} (min) (±S.D.)	$AUC_{0-240\ min}$ (±S.D.)	Relative % AUC of control
0	4	1977 ± 952	9 ± 5	55937 ± 27652	100
300	5	2107 ± 729	6 ± 3	90507 ± 22874	161.8
1000	6	4538 ± 1390	13 ± 10	292271 ± 67313	522.5

C_{max}, T_{max}, $AUC_{0-240\ min}$, and relative % of AUC to control for sCT are shown.

4. Discussion

Barrier function is a new target for drug development, drug delivery, and adjuvant development. Although the efforts to develop TJ modulators have not resulted in marketed agents to date, we are continuing to develop TJ opening molecules because of the progress in the understanding of TJ biology and the demonstration that TJs can be opened in a reversible and non-toxic manner. The discovery of ZOT protein from *V. cholerae* has allowed us to explore TJs as a drug development target. Early work showed that ZOT opened tight junctions transiently and reversibly (Karyekar et al., 2003). To avoid the technical hurdles of developing a complex protein as a drug to open TJs we are working with AT-1002, a peptide representing the first 6 amino acids of the active fragment of ZOT. This peptide retains the TJ opening properties of the parent molecule. In this paper we examined the effects of AT-1002 on epithelial cells to gain insight into the mechanism of AT-1002-induced TJ disassembly. We confirmed results from previous studies that AT-1002 caused a decrease in TEER and an increase in LY permeability across Caco-2 cell monolayers (Motlekar et al., 2006).

In this study we show that AT-1002-induced tight junction opening was accompanied by a reduced junctional distribution of ZO-1 in Caco-2 cells. This effect of AT-1002 is specific as demonstrated by the inactivity of scrambled hexapeptides tested at the same concentration. Changes in phosphorylation of TJ proteins have been implicated in the regulation of TJ function (Staddon et al., 1995; Takeda and Tsukita, 1995). Indeed, AT-1002-induced ZO-1 redistribution was accompanied by increased tyrosine phosphorylation of ZO-1. It is noteworthy that the AT-1002 induced increase in ZO-1 tyrosine phosphorylation was also reversible. Rao et al. (2002) have previously reported an increase in tyrosine phosphorylation of ZO-1 and occludin in TJ disassembly due to oxidative stress, which was shown to be mediated by src kinase (Basuroy et al., 2003). In this study we found that AT-1002 activated src kinase in Caco-2 cells. Our results also show that AT-1002 activated the MAP kinase signaling pathway. MAP kinase activation is involved in opening of TJs in response to a variety of stimuli including alcohol, oxidative stress and cytokines (reviewed in Gonzalez-Mariscal et al., 2008). In addition to tyrosine phophorylation, AT-1002 may also affect serine/threonine phosphorylation of ZO-1 because the effect of ZOT on TJs has been shown to be mediated by protein kinase C (Fasano et al., 1995).

In addition to effects on TJs, AT-1002 also caused rearrangement of actin stress fibers in Caco-2 and IEC6 cells. Interestingly, activation of src and MAP kinases has also been shown to cause actin rearrangement (Barros and Marshall, 2005; Brandt et al., 2002; Pichon et al., 2004; Rennefahrt et al., 2002). TJ structure and function are regulated by the perijunctional actomyosin ring (reviewed in Turner, 2000). TJs interface not only with the perijunctional actin ring, but also with stress fibers that emanate from this actin ring. Stress fibers have been shown to be involved in regulation of TJ assembly and function (Rajasekaran et al., 2001). AT-1002-induced stress fiber disassembly was accompanied by actin bundling at the cell periphery in IEC6 cells, but not in Caco-2 cells. However, increased TJ permeability in the absence of any change in the perijunctional actin ring is not unprecedented. In retinal pigment epithelial cells inhibition of Na-K-ATPase increased TJ permeability without altering the circumferential actin ring (Rajasekaran et al., 2003). Interestingly, in these cells increased permeability was associated with reduced actin stress fibers. Disassembly of actin stress fibers and an increase in TJ permeability in response to AT-1002 suggest the possibility that AT-1002 may inhibit Na-K-ATPase and Rho-GTPase in Caco-2 cells.

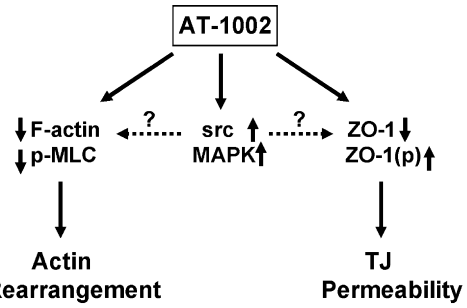

Fig. 9. A model for AT-1002-induced actin rearrangement and TJ disassembly. AT-1002 induces actin rearrangement and TJ permeability by causing F-actin disassembly, pMLC redistribution, tyrosine phosphorylation and redistribution of ZO-1. These effects may be mediated by AT-1002-induced src and MAP kinase pathways (indicated by broken arrows).

The biological effects of AT-1002 described above are depicted in the form of a model in Fig. 9. Experiments are in progress to understand how AT-1002 activates src and MAPK to affect the cytoskeleton and the levels of ZO-1 phosphorylation and redistribution. Other experiments are underway to bridge the gaps between src, MAPK and the changes to the cytoskeleton and ZO-1. Furthermore, we have identified candidate receptors for AT-1002 and experiments are underway to more fully characterize the signaling pathways that participate in AT-1002-induced disassembly of TJs (Somerville et al., in preparation).

The requirement for a high concentration of AT-1002 in this study is in contrast to a previous report (Motlekar et al., 2006). This group has reported a 2.1-fold enhanced permeability of ^{3}H-ardeparin in Caco-2 cells using a lower concentration (0.25 mg/ml) of AT-1002. This discrepancy can be explained by the difference in the method employed for permeability measurement (radioactive vs fluorimetric). In addition, the Caco-2 cell clone used, its state of differentiation and relative TEER at the time of measurements differ significantly. We selected a concentration of 5 mg/ml for our assays because it gave us the most robust, reliable and reproducible permeability enhancement, as well as the best effect on functional assays without being cytotoxic. Additionally, two scrambled versions of AT-1002 and two other unrelated 6-mer peptides did not enhance the permeability of Caco-2 cells, confirming that the permeability enhancement caused by 5 mg/ml of AT-1002 was not due to non-specific effects.

Drug absorption is thought to occur predominantly via passive transcellular and paracellular transport mechanisms (Behrens et al., 2001). Lipophilic drugs are transported primarily by the transcellular route and by means of transporters such as channels, pumps and carriers on the plasma membrane. However, the paracellular route is usually the main route of absorption for hydrophilic drugs (proteins, peptides, etc.). Here we confirm that AT-1002, a small peptide derived from ZOT, causes opening of the TJs of a Caco-2 cell monolayer (Motlekar et al., 2006; Song et al., 2008a) and show that this effect is reversible. Additional experiments showed that co-administration of AT-1002 with salmon calcitonin intratracheally increased the systemic exposure of salmon calcitonin by up to 5.2-fold suggesting that we can use AT-1002 to deliver antigens and other payloads systemically. In fact, previous studies have shown that AT-1002 enhances the delivery of small molecules (Motlekar et al., 2006; Song et al., 2008a, 2008b). Another study showed that peptides from the extracellular loops of the TJ protein occludin could be used for TJ modulation (Tavelin et al., 2003) by increasing the permeability of the TJs without causing short-term toxicity. However, these peptides had an effect only when added to the basolateral side of the monolayer. Agents that enhance drug or antigen delivery have to be applied to the apical side of epithelial surfaces

to be useful. Here we show that AT-1002 is such an agent and thus represents a prototype of a new class of TJ modulators.

Two main applications of TJ-opening molecules such as AT-1002 can be envisioned: classical drug delivery and antigen delivery for vaccination. Recently, a peptide from the capsid of rotaviruses was shown to facilitate insulin uptake in rats (Nava et al., 2004). Other TJ-modulating (TJM) peptides and peptide YY (PYY) improved drug transfer across epithelial tissues (Chen et al., 2006; Gonzalez-Mariscal and Nava, 2005). Therefore, compounds that enable efficient, non-toxic and non-invasive drug delivery would revolutionize the treatment of multiple diseases. Thus, a TJ-modulating peptide such as AT-1002 represents a promising advancement in mucosal drug delivery.

Acknowledgements

We thank Alkermes for performing the salmon calcitonin experiments reported in this study, and Drs. Alessio Fasano and Linda Arterburn for critical reading of the manuscript.

References

Aijaz, S., Balda, M.S., Matter, K., 2006. Tight junctions: molecular architecture and function. Int. Rev. Cytol. 248, 261–298.

Anderson, J.M., Van Itallie, C.M., 1995. Tight junctions and the molecular basis for regulation of paracellular permeability. Am. J. Physiol. 269, G467–475.

Artursson, P., 1990. Epithelial transport of drugs in cell culture. I. A model for studying the passive diffusion of drugs over intestinal absorptive (Caco-2) cells. J. Pharm. Sci. 79, 476–482.

Balda, M.S., Gonzalez-Mariscal, L., Contreras, R.G., Macias-Silva, M., Torres-Marquez, M.E., Garcia-Sainz, J.A., Cereijido, M., 1991. Assembly and sealing of tight junctions: possible participation of G-proteins, phospholipase C, protein kinase C and calmodulin. J. Membr. Biol. 122, 193–202.

Barros, J.C., Marshall, C.J., 2005. Activation of either ERK1/2 or ERK5 MAP kinase pathways can lead to disruption of the actin cytoskeleton. J. Cell Sci. 118, 1663–1671.

Basuroy, S., Sheth, P., Kuppuswamy, D., Balasubramanian, S., Ray, R.M., Rao, R.K., 2003. Expression of kinase-inactive c-Src delays oxidative stress-induced disassembly and accelerates calcium-mediated reassembly of tight junctions in the Caco-2 cell monolayer. J. Biol. Chem. 278, 11916–11924.

Baudry, B., Fasano, A., Ketley, J., Kaper, J.B., 1992. Cloning of a gene (zot) encoding a new toxin produced by *Vibrio cholerae*. Infect. Immun. 60, 428–434.

Behrens, I., Stenberg, P., Artursson, P., Kissel, T., 2001. Transport of lipophilic drug molecules in a new mucus-secreting cell culture model based on HT29-MTX cells. Pharm. Res. 18, 1138–1145.

Brandt, D., Gimona, M., Hillmann, M., Haller, H., Mischak, H., 2002. Protein kinase C induces actin reorganization via a Src- and Rho-dependent pathway. J. Biol. Chem. 277, 20903–20910.

Bruewer, M., Luegering, A., Kucharzik, T., Parkos, C.A., Madara, J.L., Hopkins, A.M., Nusrat, A., 2003. Proinflammatory cytokines disrupt epithelial barrier function by apoptosis-independent mechanisms. J. Immunol. 171, 6164–6172.

Cammish, L.E., Kates, S.A., 2000. In: Chan, W.C., White, P.D. (Eds.), Fmoc Solid Phase Peptide Synthesis: A Practical Approach. Oxford University Press, Oxford, pp. 277–279.

Chen, S.C., Eiting, K., Cui, K., Leonard, A.K., Morris, D., Li, C.Y., Farber, K., Sileno, A.P., Houston Jr., M.E., Johnson, P.H., Quay, S.C., Costantino, H.R., 2006. Therapeutic utility of a novel tight junction modulating peptide for enhancing intranasal drug delivery. J. Pharm. Sci. 95, 1364–1371.

Chen, Y., Lu, Q., Schneeberger, E.E., Goodenough, D.A., 2000. Restoration of tight junction structure and barrier function by down-regulation of the mitogen-activated protein kinase pathway in ras-transformed Madin-Darby canine kidney cells. Mol. Biol. Cell 11, 849–862.

De Magistris, M.T., 2006. Zonula occludens toxin as a new promising adjuvant for mucosal vaccines. Vaccine 24 (Suppl. 2), S2-60-61.

Di Pierro, M., Lu, R., Uzzau, S., Wang, W., Margaretten, K., Pazzani, C., Maimone, F., Fasano, A., 2001. Zonula occludens toxin structure-function analysis. Identification of the fragment biologically active on tight junctions and of the zonulin receptor binding domain. J. Biol. Chem. 276, 19160–19165.

Fasano, A., Baudry, B., Pumplin, D.W., Wasserman, S.S., Tall, B.D., Ketley, J.M., Kaper, J.B., 1991. *Vibrio cholerae* produces a second enterotoxin, which affects intestinal tight junctions. Proc. Natl. Acad. Sci. USA 88, 5242–5246.

Fasano, A., Fiorentini, C., Donelli, G., Uzzau, S., Kaper, J.B., Margaretten, K., Ding, X., Guandalini, S., Comstock, L., Goldblum, S.E., 1995. Zonula occludens toxin modulates tight junctions through protein kinase C-dependent actin reorganization, in vitro. J. Clin. Invest. 96, 710–720.

Fasano, A., Uzzau, S., 1997. Modulation of intestinal tight junctions by Zonula occludens toxin permits enteral administration of insulin and other macromolecules in an animal model. J. Clin. Invest. 99, 1158–1164.

Furuse, M., Hirase, T., Itoh, M., Nagafuchi, A., Yonemura, S., Tsukita, S., Tsukita, S., 1993. Occludin: a novel integral membrane protein localizing at tight junctions. J. Cell. Biol. 123, 1777–1788.

Furuse, M., Sasaki, H., Fujimoto, K., Tsukita, S., 1998. A single gene product, claudin-1 or -2, reconstitutes tight junction strands and recruits occludin in fibroblasts. J. Cell. Biol. 143, 391–401.

Ginski, M.J., Polli, J.E., 1999. Prediction of dissolution-absorption relationships from a dissolution/Caco-2 system. Int. J. Pharm. 177, 117–125.

Gonzalez-Mariscal, L., Nava, P., 2005. Tight junctions, from tight intercellular seals to sophisticated protein complexes involved in drug delivery, pathogens interaction and cell proliferation. Adv. Drug. Deliv. Rev. 57, 811–814.

Gonzalez-Mariscal, L., Tapia, R., Chamorro, D., 2008. Crosstalk of tight junction components with signaling pathways. Biochim. Biophys. Acta 1778, 729–756.

Hartsock, A., Nelson, W.J., 2008. Adherens and tight junctions: structure, function and connections to the actin cytoskeleton. Biochim. Biophys. Acta 1778, 660–669.

Haskins, J., Gu, L., Wittchen, E.S., Hibbard, J., Stevenson, B.R., 1998. ZO-3, a novel member of the MAGUK protein family found at the tight junction, interacts with ZO-1 and occludin. J. Cell. Biol. 141, 199–208.

Hochman, J., Artursson, P., 1994. Mechanisms of absorption enhancement and tight junction regulation. J. Control Release 29, 253–267.

Karyekar, C.S., Fasano, A., Raje, S., Lu, R., Dowling, T.C., Eddington, N.D., 2003. Zonula occludens toxin increases the permeability of molecular weight markers and chemotherapeutic agents across the bovine brain microvessel endothelial cells. J. Pharm. Sci. 92, 414–423.

Kondoh, M., Yagi, K., 2007. Progress in absorption enhancers based on tight junction. Expert. Opin. Drug Deliv. 4, 275–286.

Lee, A., White, N., van der Walle, C.F., 2003. The intestinal zonula occludens toxin (ZOT) receptor recognises non-native ZOT conformers and localises to the intercellular contacts. FEBS Lett. 555, 638–642.

Li, M., Oliver, E., Kitchens, K.M., Vere, J., Alkan, S.S., Tamiz, A.P., 2008. Structure-activity relationship studies of permeability modulating peptide AT-1002. Bioorg. Med. Chem. Lett. 18 (16), 4584–4586.

Marinaro, M., Di Tommaso, A., Uzzau, S., Fasano, A., De Magistris, M.T., 1999. Zonula occludens toxin is a powerful mucosal adjuvant for intranasally delivered antigens. Infect. Immun. 67, 1287–1291.

Marinaro, M., Fasano, A., De Magistris, M.T., 2003. Zonula occludens toxin acts as an adjuvant through different mucosal routes and induces protective immune responses. Infect. Immun. 71, 1897–1902.

Martin-Padura, I., Lostaglio, S., Schneemann, M., Williams, L., Romano, M., Fruscella, P., Panzeri, C., Stoppacciaro, A., Ruco, L., Villa, A., Simmons, D., Dejana, E., 1998. Junctional adhesion molecule, a novel member of the immunoglobulin superfamily that distributes at intercellular junctions and modulates monocyte transmigration. J. Cell. Biol. 142, 117–127.

Matter, K., Balda, M.S., 1998. Biogenesis of tight junctions: the C-terminal domain of occludin mediates basolateral targeting. J. Cell. Sci. 111 (Pt 4), 511–519.

Motlekar, N.A., Fasano, A., Wachtel, M.S., Youan, B.B., 2006. Zonula occludens toxin synthetic peptide derivative AT1002 enhances in vitro and in vivo intestinal absorption of low molecular weight heparin. J. Drug Target 14, 321–329.

Nash, S., Stafford, J., Madara, J.L., 1988. The selective and superoxide-independent disruption of intestinal epithelial tight junctions during leukocyte transmigration. Lab. Invest. 59, 531–537.

Nava, P., Lopez, S., Arias, C.F., Islas, S., Gonzalez-Mariscal, L., 2004. The rotavirus surface protein VP8 modulates the gate and fence function of tight junctions in epithelial cells. J. Cell. Sci. 117, 5509–5519.

Patrick, D.M., Leone, A.K., Shellenberger, J.J., Dudowicz, K.A., King, J.M., 2006. Proinflammatory cytokines tumor necrosis factor-alpha and interferon-gamma modulate epithelial barrier function in Madin-Darby canine kidney cells through mitogen activated protein kinase signaling. BMC Physiol. 6, 2.

Pichon, S., Bryckaert, M., Berrou, E., 2004. Control of actin dynamics by p38 MAP kinase - Hsp27 distribution in the lamellipodium of smooth muscle cells. J. Cell. Sci. 117, 2569–2577.

Rajasekaran, S.A., Hu, J., Gopal, J., Gallemore, R., Ryazantsev, S., Bok, D., Rajasekaran, A.K., 2003. Na, K-ATPase inhibition alters tight junction structure and permeability in human retinal pigment epithelial cells. Am. J. Physiol. Cell. Physiol. 284, C1497–1507.

Rajasekaran, S.A., Palmer, L.G., Quan, K., Harper, J.F., Ball Jr., W.J., Bander, N.H., Peralta Soler, A., Rajasekaran, A.K., 2001. Na, K-ATPase beta-subunit is required for epithelial polarization, suppression of invasion, and cell motility. Mol. Biol. Cell 12, 279–295.

Rao, R.K., Basuroy, S., Rao, V.U., Karnaky Jr., K.J., Gupta, A., 2002. Tyrosine phosphorylation and dissociation of occludin-ZO-1 and E-cadherin-beta-catenin complexes from the cytoskeleton by oxidative stress. Biochem. J. 368, 471–481.

Rennefahrt, U.E., Illert, B., Kerkhoff, E., Troppmair, J., Rapp, U.R., 2002. Constitutive JNK activation in NIH 3T3 fibroblasts induces a partially transformed phenotype. J. Biol. Chem. 277, 29510–29518.

Salama, N.N., Eddington, N.D., Fasano, A., 2006. Tight junction modulation and its relationship to drug delivery. Adv. Drug. Deliv. Rev. 58, 15–28.

Salama, N.N., Fasano, A., Thakar, M., Eddington, N.D., 2004. The effect of delta G on the transport and oral absorption of macromolecules. J. Pharm. Sci. 93, 1310–1319.

Salama, N.N., Fasano, A., Thakar, M., Eddington, N.D., 2005. The impact of DeltaG on the oral bioavailability of low bioavailable therapeutic agents. J. Pharmacol. Exp. Ther. 312, 199–205.

Schmidt, E., Kelly, S.M., van der Walle, C.F., 2007. Tight junction modulation and biochemical characterisation of the zonula occludens toxin C-and N-termini. FEBS Lett. 581, 2974–2980.

Schneeberger, E.E., Lynch, R.D., 2004. The tight junction: a multifunctional complex. Am. J. Physiol. Cell. Physiol. 286, C1213–1228.

Shen, T.Y., Qin, H.L., Gao, Z.G., Fan, X.B., Hang, X.M., Jiang, Y.Q., 2006. Influences of enteral nutrition combined with probiotics on gut microflora and barrier function of rats with abdominal infection. World J. Gastroenterol. 12, 4352–4358.

Sheth, P., Basuroy, S., Li, C., Naren, A.P., Rao, R.K., 2003. Role of phosphatidylinositol 3-kinase in oxidative stress-induced disruption of tight junctions. J. Biol. Chem. 278, 49239–49245.

Song, K.H., Fasano, A., Eddington, N.D., 2008a. Enhanced nasal absorption of hydrophilic markers after dosing with AT1002, a tight junction modulator. Eur. J. Pharm. Biopharm. 69 (1), 231–237.

Song, K.H., Fasano, A., Eddington, N.D., 2008b. Effect of the six-mer synthetic peptide (AT1002) fragment of zonula occludens toxin on the intestinal absorption of cyclosporin A. Int. J. Pharm. 351, 8–14.

Staddon, J.M., Herrenknecht, K., Smales, C., Rubin, L.L., 1995. Evidence that tyrosine phosphorylation may increase tight junction permeability. J. Cell Sci. 108 (Pt 2), 609–619.

Stevenson, B.R., Siliciano, J.D., Mooseker, M.S., Goodenough, D.A., 1986. Identification of ZO-1: a high molecular weight polypeptide associated with the tight junction (zonula occludens) in a variety of epithelia. J. Cell Biol. 103, 755–766.

Takeda, H., Tsukita, S., 1995. Effects of tyrosine phosphorylation on tight junctions in temperature-sensitive v-src-transfected MDCK cells. Cell Struct. Funct. 20, 387–393.

Tavelin, S., Hashimoto, K., Malkinson, J., Lazorova, L., Toth, I., Artursson, P., 2003. A new principle for tight junction modulation based on occludin peptides. Mol. Pharmacol. 64, 1530–1540.

Turner, J.R., 2000. 'Putting the squeeze' on the tight junction: understanding cytoskeletal regulation. Semin. Cell. Dev. Biol. 11, 301–308.

Turner, J.R., 2006. Molecular basis of epithelial barrier regulation: from basic mechanisms to clinical application. Am. J. Pathol. 169, 1901–1909.

Weber, C.R., Turner, J.R., 2007. Inflammatory bowel disease: is it really just another break in the wall? Gut 56, 6–8.